

# *In situ* high $P$ - $T$ Raman spectroscopy and laser heating of carbon dioxide

Mario Santoro,<sup>a)</sup> Jung-fu Lin, Ho-kwang Mao, and Russell J. Hemley  
*Geophysical Laboratory, Carnegie Institution of Washington, Washington, D.C. 20015*

(Received March 31 2004; accepted April 14 2004)

*In situ* high  $P$ - $T$  Raman spectra of solid CO<sub>2</sub> up to 67 GPa and 1660 K have been measured, using a micro-optical spectroscopy system coupled with a Nd:YLF laser heating system in diamond anvil cells. A metallic foil was employed to efficiently absorb the incoming Nd:YLF laser and heat the sample. The average sample temperature was accurately determined by detailed balance from the anti-Stokes/Stokes ratio, and was compared to the temperature of the absorber determined by fitting the thermal radiation spectrum to the Planck radiation law. The transformation temperature threshold and the transformation dynamics from the molecular phases III and II to the polymeric phase V, previously investigated only by means of temperature quench experiments, was determined at different pressures. The  $P$ - $T$  range of the transformation, between 640 and 1100 K in the 33–65 GPa pressure interval, was assessed to be a kinetic barrier rather than a phase boundary. These findings lead to a new interpretation of the high  $P$ - $T$  phase diagram of carbon dioxide. Furthermore, our approach opens a new way to perform quantitative *in situ* Raman measurements under extremely high pressures and temperatures, providing unique information about phase relations and structural and thermodynamic properties of materials under these conditions. © 2004 American Institute of Physics. [DOI: 10.1063/1.1758936]

## I. INTRODUCTION

High pressure techniques provide the leading tool to strongly modify and investigate molecular interactions in simple molecular solids. These interactions become highly repulsive at high density, mainly due to the kinetic energy of the electrons. Solid-solid phase transitions thus occur to minimize the overall energy of the system. Particularly dramatic changes can take place when intermolecular and intramolecular distances converge, a situation with profound effects on chemical bonds. In this respect a variety of transformations have been observed, including the insulator to metal transitions [O<sub>2</sub> (Ref. 1), I<sub>2</sub> (Ref. 2), Xe (Ref. 3)], molecular transformations [O<sub>2</sub> (Ref. 4)], and polymerization and amorphization of simple organic compounds [C<sub>2</sub>H<sub>2</sub> (Ref. 5), C<sub>4</sub>H<sub>6</sub> (Ref. 6), C<sub>6</sub>H<sub>6</sub> (Ref. 7)].

The role of high temperature is of paramount importance in discovering possible new high  $P$ - $T$  phases of simple molecular systems, and/or overcoming the kinetic barriers which often hinder the high density transformations. Also, high  $P$ - $T$  methods give appealing perspectives to planetary science. Shock wave techniques provide methods for accessing extreme high  $P$ - $T$  conditions and have thus revealed crucial information.<sup>8</sup> Nevertheless, some drawbacks related to these experiments have to be pointed out: temperature and pressure are coupled in these transient experiments, and the employment of *in situ* techniques is limited. On the other hand, recent developments in laser heating/diamond anvil cell (DAC) techniques provide access to high  $P$ - $T$  condition with available static *in situ* probes of the structural and dy-

namical properties.<sup>9,10</sup> The laser-heated DAC technique has been widely used with *in situ* x-ray diffraction to study the crystal structure, phase diagrams, and thermal equations of state of materials under the  $P$ - $T$  conditions of the Earth's interior. However, this technique has been rarely applied to investigating important planetary/molecular systems containing low- $Z$  elements and compounds under extreme conditions. Because these systems can have high Raman cross section, *in situ* Raman studies by laser heating may be employed to investigate their physical properties.

In this work we investigate the high  $P$ - $T$  transformations of solid CO<sub>2</sub> by means of *in situ* Raman spectroscopy on laser-heated samples in the DAC. Carbon dioxide is one of the most important volatile systems. It is the dominant component of the atmospheres of terrestrial planets such as Mars and Venus, is commonly found in ice form in planets and asteroids, and is an important volatile in volcanic activity. From the fundamental point of view it is one of the model systems involving the  $\pi$  bonding and the hybridization properties of the carbon atom, which are strongly affected by the high pressure conditions. Despite its simplicity, carbon dioxide undergoes a number of high pressure modifications, also involving strong metastabilities. At room temperature CO<sub>2</sub> solidifies into cubic phase I (known as dry ice,  $Pa3$ ) with strong double bonds and rather weak intermolecular interaction.<sup>11</sup> Furthermore, CO<sub>2</sub>-I transforms to orthorhombic phase III ( $Cmca$ ) between 12 and 22 GPa.<sup>12–18</sup> The I-III transition is sluggish at ambient temperature, but is strongly temperature dependent, occurring abruptly above 400 K as found by Iota and Yoo.<sup>19</sup> The structural investigation of phase III was performed up to 60 GPa by Yoo *et al.*<sup>12</sup> There it was shown that the I-III transition occurs with no apparent volume discontinuity, and the orthorhombic  $Cmca$  structure of CO<sub>2</sub>-III was confirmed in the whole pressure range inves-

<sup>a)</sup>Permanent address: LENS, European Laboratory for Non Linear Spectroscopy and INFN, Via Carrara 1, I-50019 Sesto Fiorentino, Firenze, Italy. Electronic mail: m.santoro@gl.ciw.edu; santoro@lens.unifi.it

tigated. In addition, they reported large pressure gradients in phase III (100–200 GPa/mm above 30 GPa), an unusually high bulk modulus, equal to 87 GPa, and collapsed intermolecular distances. So the authors concluded that CO<sub>2</sub>-III is a high strength material with increased intermolecular bonding, implying that CO<sub>2</sub>-III is not entirely molecular. Finally, only one  $P$ - $T$  path was found to produce CO<sub>2</sub>-III: phase III appeared only via low temperature compression of phase I.<sup>19</sup> On the basis of such observations CO<sub>2</sub>-III was suggested to be a metastable phase.

A nonmolecular solid phase of carbon dioxide (phase V) was synthesized in the DAC by laser heating of phase III above 40 GPa and 1800 K.<sup>20</sup> This material was quenched to ambient temperature and was recovered down to 1 GPa. The Raman spectrum showed a strong peak in the 700–800 cm<sup>-1</sup> spectral range which was assigned to the symmetric stretch of the C-O-C bonds, thus indicating the formation of an extended covalent solid with carbon-oxygen single bonds similar to the quartz polymorph of SiO<sub>2</sub>. This material was also found to exhibit nonlinear optical properties, generating the second harmonic of a near infrared light beam. The observed  $P$ - $T$  transition boundary was argued to represent a kinetic barrier rather than the thermodynamic phase boundary. The x-ray diffraction investigation, together with *ab initio* simulations, led to the assignment of the tridymite structure ( $P2_12_12_1$ ) to phase V and to the determination of a 15.3% volume reduction with respect to phase III above 40 GPa.<sup>12</sup> Each carbon atom of CO<sub>2</sub>-V is tetrahedrally bonded with four oxygen atoms. This phase is likely superhard with a high incompressibility of 365 GPa, similar to cubic BN. The high pressure transformation of carbon dioxide to a nonmolecular phase involving special arrangements of CO<sub>4</sub> tetrahedra has also been examined theoretically by different authors,<sup>21–23</sup> but the results differ. In the experimental studies,<sup>20,12</sup> some important limitations affected the full determination of the thermodynamic properties of the III to V transformation and of phase V itself: (1) Raman spectra and diffraction patterns were measured only on the temperature quenched material, (2) the temperature threshold was roughly estimated by the gray-body radiation of an optical absorber employed to heat the sample indirectly, and (3) the overall metastable character, instead of stable, of the synthesized material at room temperature was just claimed.

Laser heating of solid CO<sub>2</sub> at 30–80 GPa and 3000–1500 K resulted in the breakdown of this compound to molecular oxygen and diamond.<sup>24</sup> Above 40 GPa the decomposition was preceded by the formation of a new nonmolecular CO<sub>2</sub> phase (CO<sub>2</sub>-VI). Also in this case, the limitation of spectroscopic and diffraction data to the temperature quenched material and the very rough estimation of the transformation temperatures led to only an approximate kinetic (as opposed to thermodynamic) phase diagram. Decomposition of carbon dioxide was also found in shock wave measurements above 34 GPa where the calculated temperature was estimated to be 4500 K.<sup>25</sup>

Recently two new solid phases, CO<sub>2</sub>-IV and II, both produced at high temperature, were discovered and suggested to be intermediate between molecular and covalent-bonded solids.<sup>19,26–28</sup> Phase IV was obtained by heating

CO<sub>2</sub>-III between 12 and 30 GPa and shown to be nonlinear (bent), due to the activation of the forbidden bending mode of CO<sub>2</sub> in the Raman spectrum.<sup>26</sup> This phase was quenched at room temperature and shown to persist between 12 and 80 GPa, bypassing the entire field of phase III. Laser heating of quenched phase IV further transformed it to phase V above 30 GPa. At 80 GPa, CO<sub>2</sub>-IV became an extended amorphous solid. Two plausible crystal structures of phase IV were proposed with bent C=O=C molecules: tetragonal  $P4_12_12$  and orthorhombic  $Pbcn$ .<sup>28</sup> The volume of this solid was found to be very close to that of phase III. Furthermore, the intramolecular (intermolecular) CO distance was found to be strongly increased (decreased), thus pointing to an increased intermolecular interaction and to the character of phase IV as a precursor to forming the covalent phase V. Phase II was achieved by heating CO<sub>2</sub>-III above 20 GPa and 500 K and was quenched to ambient temperature. The Raman spectrum was interpreted as indicating pairing of molecules. The crystal structure of phase II was determined to be tetragonal  $P4_2/mnm$  with some evidence of tetragonal-to-orthorhombic ( $Pnmm$ ) disorder. As in phase IV, but at a lower grade here, elongated C=O distances and collapsed intermolecular separations pointed to strong intermolecular association and to the precursor character for forming phase V. Phase II is about 5%–7% denser than CO<sub>2</sub>-III. It is reported to have an unusually high bulk modulus equal to 131.5 GPa.<sup>27</sup>

In a recent paper by Bonev *et al.*<sup>29</sup> the structure and the relative stability of phase I, II, III, and IV were reexamined by first-principles calculations. The authors confuted the concept of intermediate phases belonging to CO<sub>2</sub>-IV and II, and proposed instead molecular structures, providing a very good agreement with measurements. Here the structure  $P4_2/mnm$  was assigned to phase II, and the C=O bond length was found to be comparable to the free CO<sub>2</sub> molecule. This structure was also found to be stable over the entire range of phase III, thus confirming that CO<sub>2</sub>-III is a metastable phase. The structure  $Cmca$ , previously assigned to CO<sub>2</sub>-III, was reassigned to phase IV. Finally, the high bulk moduli found for phases III and II (Refs. 12, 27) were calculated to be two orders of magnitude smaller, a discrepancy ascribed to an incorrect extrapolation of the experimental data to ambient pressure.

By comparing all the above-mentioned findings, the topic of high  $P$ - $T$  solid carbon dioxide appears still controversial. In this work we investigate the pressure-temperature range between 10–67 GPa and 300–1700 K, respectively. A specific attempt was made to observe, by means of *in situ* Raman spectroscopy, the onset of the formation and the stability of nonmolecular carbon dioxide from the molecular phases. In addition, the average temperature determined from the detailed Stokes/anti-Stokes balance of the Raman spectrum was ascribed to the actual temperature of the laser-heated sample itself. These measurements have led us to revise the high  $P$ - $T$  phase diagram of carbon dioxide.

## II. EXPERIMENTAL PROCEDURE

Carbon dioxide was loaded in a symmetric DAC by means of the gas loading technique. The gaseous CO<sub>2</sub> was

compressed to about 1800 bar and then sealed in the DAC. As shown by the Raman spectrum, the sample was fully transformed into phase III above 30 GPa in compression. The highly textured morphology of this phase was also observed. To determine the temperature transformation threshold from molecular solid carbon dioxide to the covalent solid, different samples were systematically laser heated at pressures in the 30–67 GPa range. Pressure was determined by the ruby luminescence technique<sup>30</sup> at room temperature before and after each heating cycle.

A Nd:YLF laser, with a maximum power of 80 W and spot size of about 40  $\mu\text{m}$  at the sample surface, was used to heat the sample from one side. Type I diamond anvils were employed with culet sizes between 400 and 250  $\mu\text{m}$ . A rhenium gasket was preindented to 25–30  $\mu\text{m}$  and a hole of 100–150  $\mu\text{m}$  in diameter was drilled in it. A thin metallic (Re or Pt) foil having thicknesses of 5 to 20  $\mu\text{m}$  was put into the sample chamber to absorb the laser energy and heat the  $\text{CO}_2$  sample. We used the metallic foil as an internal heating furnace because of the transparency of the sample to the laser wavelength (1053 nm). A small hole, 10–20  $\mu\text{m}$  in diameter, was drilled through the foil and the sample was uniformly heated here, and Raman spectra were collected *in situ*. The temperature of the foil was determined by fitting the gray-body thermal radiation spectrum between 670 nm and 830 nm to the Planck radiation function. However, this is not a direct probe of the actual sample temperature, being the sample thermal emission far away from that of the metallic coupler and specifically much lower than it is. Consequently we used the temperatures determined from the principle of detailed balance applied to the Raman spectrum (see below) as the average sample temperature during the heating. We did not employ any insulating layer between sample and anvils in order to avoid effects of any possible chemical reaction. This choice limited the actual temperatures below 1700 K.

The 488 nm line of an  $\text{Ar}^+$  laser was employed as Raman excitation source, with a typical input power of several tenths of a Watt. The  $\text{Ar}^+$  and Nd:YLF lasers were focused into the sample chamber from opposite sides in a confocal configuration. The spot size of the argon laser was equal to a few microns; the high throughput-single grating Jobin-Yvon HR460 monochromator and a charge-coupled device (CCD) detector were used to disperse and detect the scattered light, respectively. The Raman spectra were measured in back-scattering geometry. Two holographic notch filters, in cascade, were employed to cut off the Rayleigh line and simultaneously measure the Stokes and the anti-Stokes bands. Both the external and internal vibrational frequency regions of the molecular crystal were measured above 10 GPa and temperatures of the metal foil as high as 2000 K. The Stokes/anti-Stokes detailed balance was performed on both kinds of excitation. The actual sample temperature is obtained from the relationship:  $I_{aS}/I_S = \beta(E)\exp(-E/k_B T)$ , where  $I_{aS}$  and  $I_S$  are the intensities of an anti-Stokes/Stokes pair,  $E$  is the energy of the Raman transition,  $k_B$  is the Boltzmann constant,  $T$  is the temperature, and  $\beta(E)$  is a factor related to the cross sections ratio. The value of the ratio  $I_{aS}/I_S$  is obtained by the measured intensities, after having corrected them by

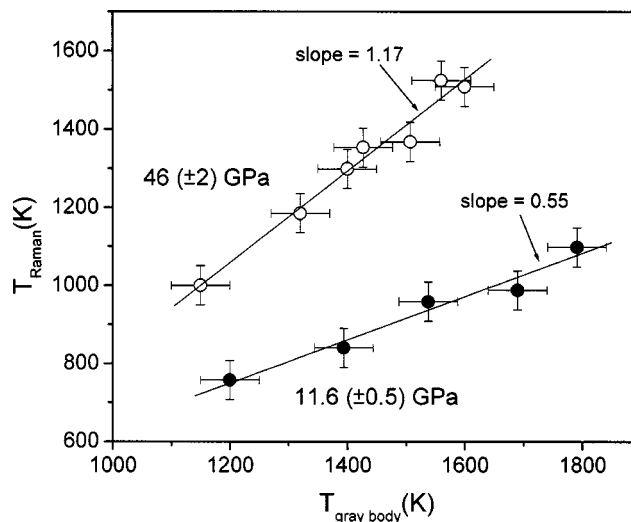


FIG. 1. Averaged sample temperature determined by the detailed balance principle,  $T_{\text{Raman}}$ , vs that obtained from the thermal radiation spectrum of the metal foil (Pt),  $T_{\text{gray-body}}$ , (see text) at two different pressures: 46 GPa (open dots) and 11.6 GPa (full dots). The integration times employed to acquire both the Raman and the thermal emission spectra were typically around 5–10 s. Error bars on  $T_{\text{Raman}}$ ,  $\pm 50$  K were estimated combining the inaccuracy related to the actual spectra and the calibration procedure.  $T_{\text{gray-body}}$  was determined just before and after having collected each Raman spectrum, and related error bars, amounting to  $\pm 50$  K, are mainly due to the difference between the two measurements. At 11.6 GPa  $T_{\text{Raman}}$  was evaluated from the pair of peaks assigned to the molecular symmetric stretching mode, positioned around  $\pm 1416 \text{ cm}^{-1}$ , which by far is the most intense spectral feature at this pressure. At 46 GPa several pairs of phonon lines were available to determine  $T_{\text{Raman}}$  (see Fig. 3). The results obtained from different pairs agree within the reported error bars. The agreement between  $T_{\text{Raman}}$  and  $T_{\text{gray-body}}$  increases as the pressure is raised due to the increased thermal conductivity of both the sample and the absorber.

the spectral response of the system, i.e., monochromator, CCD, and optics.

### III. RESULTS

In Fig. 1 we report the averaged sample temperature determined by the detailed balance principle,  $T_{\text{Raman}}$ , versus that obtained from the thermal radiation spectrum of the metal foil (Pt),  $T_{\text{gray-body}}$ , at two different pressures: 11.6 and 46 GPa. At 11.6 GPa the sample was heated deep inside phase IV (see the known phase diagram in Fig. 4) and this phase was quenched at room temperature. The detailed balance associated with the pair of diamond peaks along the heating run is always comparable to the value obtained at room  $T$ , indicating the very local character of the heating procedure. At 46 GPa the sample was driven from phase III into phase V, as discussed below. At 11.6 GPa  $T_{\text{gray-body}}$  is much higher than  $T_{\text{Raman}}$ , the difference between the two amounting to several hundreds of degrees. The data were fitted to a line with a slope equal to 0.55. The systematic difference between the metal foil temperature and the actual sample temperature demonstrates the necessity of measuring this last one *in situ* (e.g., from the Raman spectrum) to obtain valid results in high pressure/laser heating experiments. To our knowledge, this is the first high pressure/laser heating study, in which the absolute averaged sample temperature was obtained from the detailed balance principle, providing a

new way to quantitatively investigate the high  $P$ - $T$  properties of materials. The agreement between  $T_{\text{Raman}}$  and  $T_{\text{gray-body}}$  increases as the pressure is stepped up due to the increased thermal conductivity of both the sample and the metal foil. At 46 GPa the two temperatures are very close and the slope of the linear behavior is as high as 1.17. The high thermal conductivities also reduce the maximum temperature of the metal foil due to the increased heat losses to the diamond anvils.

We also checked the homogeneity of the room temperature quenched phase V in the sample chamber. These results revealed that temperature inhomogeneities had occurred along the heating run. The signature of phase V was present in the sample chamber confined by the metal foil and on the surface of the foil itself, where the sample thickness is as low as a few microns. On the other hand, these features sharply vanished beyond the external edge of the foil, where the spectrum can be ascribed to pure phase III, thus showing that a much lower temperature was achieved here during the heating procedure. The heat radial distribution was therefore well confined inside the metal foil area.

The dynamics of transformation of solid carbon dioxide from phase III to phase V, the corresponding onset temperature and the high temperature stability of  $\text{CO}_2$ -V were determined *in situ* here for the first time. In Fig. 2 we show selected Raman spectra measured at 36 GPa up to 910 K along a typical laser-heating run, where the Nd:YLF laser power was slowly increased, thereby allowing the accurate determination of the onset of the transformation to phase V. The reported temperatures are obtained from the Raman spectra. The duration of the whole heating cycle was as long as 10–15 min. Both the Stokes and the anti-Stokes spectral regions are reported (below the position of the diamond peak). The transition between molecular phases (III and II) to the polymeric phase V. The transition between phases III and II was observed prior to formation of phase V, as evidenced by the changes in the lattice region (features \* and \*\*). The inset shows the narrow region of the two phonon bands. The whole spectrum was decomposed into two pairs of features. One of these is comparable to the spectrum of phase III (dashed line), while the other pair (dotted line) is assigned to phase II.

almost simultaneously with the transformation from  $\text{CO}_2$ -III to  $\text{CO}_2$ -II, as shown by the modification of the features below  $400 \text{ cm}^{-1}$  and the appearance at the same time, above this frequency, of the spectrum of  $\text{CO}_2$ -V. Finally, the sample temperature was lowered down to ambient, with an overall cooling time of a few minutes. We did not observe any further transformations on the temperature quench and the spectrum at room temperature is almost identical to that reported at 910 K.

Figure 3 shows Raman spectra measured along a heating run at about 46 GPa, similar to that described above. In this case, the Nd:YLF laser power was abruptly increased; temperature jumps of several hundreds of degrees were produced in 1 to 2 s in order to detect possible changes in the kinetics of transformation to phase V. The spectra recorded at room temperature and 670 K are clearly assigned to phase III. At 1370 K the intensity of the  $\text{CO}_2$ -III spectral features is reduced to about 30% of the initial value, the peaks of phase V, centered at about 479, 807, 908, 1127, and  $1227 \text{ cm}^{-1}$  respectively, are very strong, and no signatures of phase II are detected. At 1540 K the amount of transformed phase V is just slightly increased, while the spectrum of the recovered

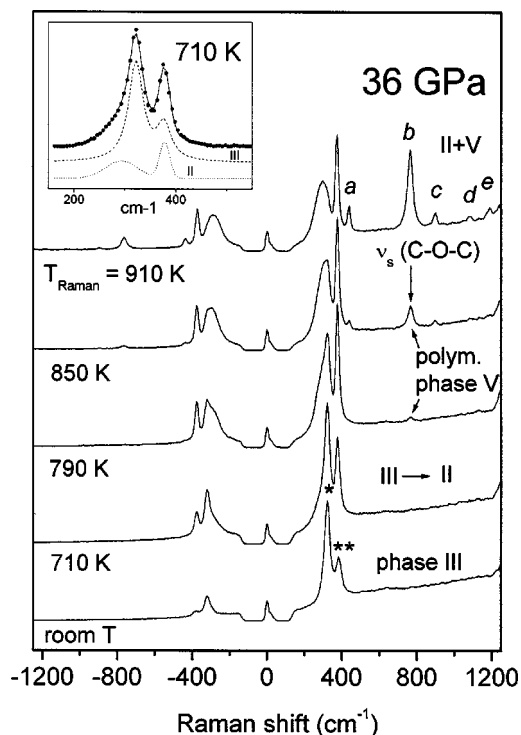


FIG. 2. Selected Raman spectra measured in a typical laser heating run. The region extending between  $-150$  and  $+150 \text{ cm}^{-1}$  was cut off by means of the notch filters as discussed in the text, and a very weak residual Rayleigh line is observed at zero frequency. The broad background extending on the Stokes side is dominated by diamond fluorescence, as the thermal emission contribution is negligible at these temperatures. Here the Nd:YLF laser power was slowly varied, thereby allowing accurate observation of the transformation from molecular phases (III and II) to the polymeric phase V. The transition between phases III and II was observed prior to formation of phase V, as evidenced by the changes in the lattice region (features \* and \*\*). The inset shows the narrow region of the two phonon bands. The whole spectrum was decomposed into two pairs of features. One of these is comparable to the spectrum of phase III (dashed line), while the other pair (dotted line) is assigned to phase II.

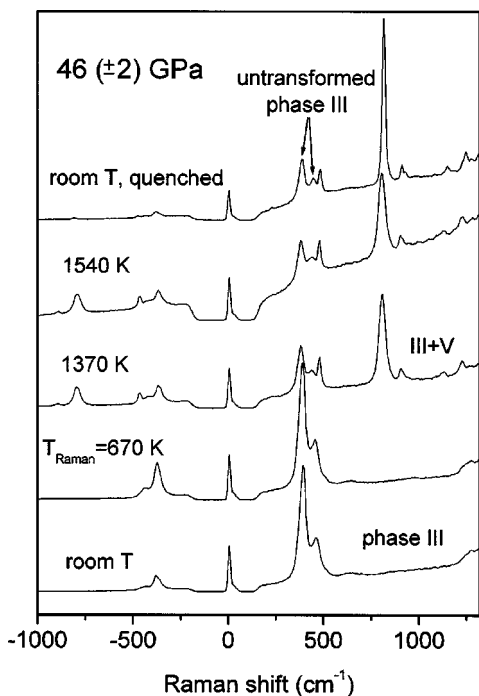


FIG. 3. Selected Raman spectra measured on heating. An increase in temperature from 670 to 1370 K led to the transformation of phase III directly to phase V. The passage through CO<sub>2</sub>-II is avoided, thus showing that this phase is not necessarily involved in the molecular transformation. The broad background is significantly increased at 1540 K due to thermal radiation.

sample at room *T* is almost unchanged apart from the strong line narrowing of the peak at 807 cm<sup>-1</sup>. A pressure drop from 48 to 44 GPa was observed during the run. This result shows that a sharp temperature increase leads to the transformation to CO<sub>2</sub>-V directly from CO<sub>2</sub>-III, without passing through phase II. On the other hand, a temperature increase in small increments, starting from room *T* at the same pressure, produced both phases V and II almost simultaneously (i.e., at the same temperature).

We determined systematically the threshold temperature for the transformation to phase V at different pressures between 33 and 65 GPa, by gradually increasing the Nd:YLF laser power as in the run reported in Fig. 2. These *P-T* points are plotted in Fig. 4 superimposed on the approximate transformation boundaries estimated previously.<sup>24,19</sup> A minimum in the transformation temperature is found between 50 and 55 GPa, equal to about 640 K. Temperature error bars are as high as ±60–150 K; they are due both to the inaccuracy in determining the Raman temperature and the uncertainty in determining the onset of the transformation. Pressure error bars range from ±1 to ±3 GPa and are due both to the large pressure gradients affecting the CO<sub>2</sub>-III solid and the pressure variation experienced during the heating run. This latter was due to two main effects: the volume variation associated with the transformation, and the mechanical instability of the whole cell assembly, which was subjected to a temperature increase of several tens of degrees. We point out that in order to minimize the inaccuracy due to the huge pressure gradients, the pressure was determined by measuring the fluorescence of small ruby chips (a few microns in diameter) placed as close as possible to the region where we collected the

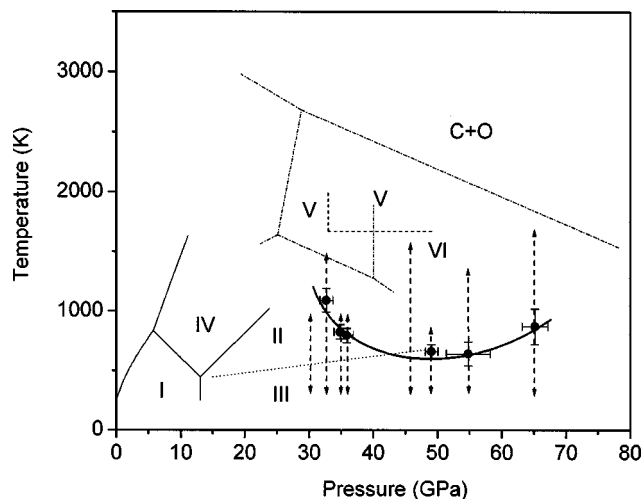


FIG. 4. Threshold temperature for the transformation to phase V (dots, this work) at different pressures, superimposed on the approximate transformation boundaries previously determined: dotted (here called line *B*), dashed, and dashed-dot lines were determined in Refs. 19, 20, and 24, respectively. The thick continuous line passing through the points (line *A*) is a guide for the eye. The boundaries lying below 20 GPa (continuous lines) are from Ref. 19. Vertical arrows indicate the heating runs performed in this work.

Raman spectrum. Detailed observation of the kinetics of transformation to phase V becomes very difficult above 60 GPa. In fact, phase III becomes amorphous upon further compression as shown by the vanishing Raman intensities. At 65 GPa the phonon peaks of CO<sub>2</sub>-III appear as a small hump hardly distinguishable from the broad luminescence background; a slightly stronger broadband is also observed around 1000 cm<sup>-1</sup> that we ascribe to the second order phonon scattering. The weakness of the Raman signal in phase III prevents accurate determination of the transition temperature, even if very sharp peaks are still observed in phase V at both high and room temperature.

In order to further clarify the phase diagram region ascribed to nonmolecular carbon dioxide and to compare our results with previous studies,<sup>19,20,24</sup> we report in Fig. 5 the pressure shift of the observed Raman peaks, assigned to CO<sub>2</sub>-V. The sample was partially transformed at about 65 GPa and 1660 K and the frequencies were evaluated on decompression from 67 GPa down to about 12 GPa at room temperature; at this pressure the crystal rapidly starts to transform back into the CO<sub>2</sub>-I molecular solid. The maximum available resolution (~2 cm<sup>-1</sup>) was employed in this case in order to observe fine details of the spectral bands. The two peaks positioned above 1000 cm<sup>-1</sup>, *d* and *e*, harden with pressure, at the same rate, and are hardly detected below 22 GPa. Peak *c*<sub>1</sub>, around 900 cm<sup>-1</sup>, is rather pressure insensitive, while frequency *c*<sub>2</sub> decreases with lowering pressure and vanishes progressively toward 43 GPa along this run. On the other hand, different runs show that *c*<sub>2</sub> becomes very close to *c*<sub>1</sub> (within about 10–15 cm<sup>-1</sup> below 40 GPa). Peak *b* is slightly asymmetric along its low frequency side, pointing to a very weak additional component which is never resolved from the main one; the frequency of the center of mass of such a band is reported in the figure. The very weak band *b'* is positioned around 750 cm<sup>-1</sup> and is no longer

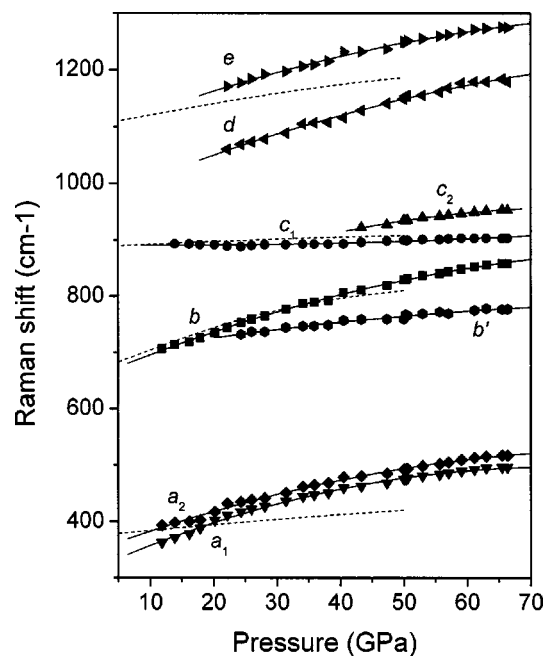


FIG. 5. Pressure dependence of the Raman frequencies observed in phase V evaluated at room temperature along a decompression path. Guides for the eye and data from Ref. 20 are also plotted (continuous and dashed lines, respectively). The comparison with previous results found by Tschauer *et al.* (Ref. 24) is discussed in the text.

detectable below 24 GPa. Two bands  $a_1$  and  $a_2$  are observed between 350 and 520  $\text{cm}^{-1}$ ; they are very close to each other, sharp and fairly well resolved at high pressure, while tending to merge in a single band with decreasing pressure. Finally, extremely weak features are observed at lower frequencies, which are assigned to the residual molecular phase.

This behavior is qualitatively in agreement with that reported by Iota *et al.*<sup>20</sup> They found shifted positions and different slopes, which we reasonably ascribe to the fact that they decompressed the sample starting from a lower pressure, 50 GPa, than we did. We suggest that the  $P$ - $T$  path does influence the actual values of the vibrational frequencies. Iota *et al.*<sup>20</sup> observed the features mentioned above, but they reported the behavior of only one band above 1000  $\text{cm}^{-1}$  and did not report the behavior of peak  $b'$ , in addition a unique frequency is given to each of the two manifolds ( $a_1, a_2$ ) and ( $c_1, c_2$ ), respectively, although the corresponding bands are clearly asymmetric and double degeneracy was assigned to them. The behavior above 1000  $\text{cm}^{-1}$  ranges between our  $d$  and  $e$  frequencies, while  $b$  and  $a$  are shifted by at most 20 and 65  $\text{cm}^{-1}$ , respectively. Different results were found by Tschauer *et al.*<sup>24</sup> by decompressing nonmolecular carbon dioxide samples which were produced at temperatures estimated above 1500 K. Peaks  $b$  and  $a$  show a discontinuity at about 40 GPa, amounting to about 50 and 20  $\text{cm}^{-1}$ , respectively. Also, an additional peak was found between band  $b$  and  $a$ , which disappears below 40 GPa.

#### IV. DISCUSSION

The transformation temperatures to nonmolecular carbon dioxide found in this work are lower than those previously

reported by means of rough evaluation methods based on the thermal emission spectrum.<sup>20,24</sup> The employment of *in situ* Raman spectroscopy to both measure accurately the sample temperature and precisely detect the onset of the transformations provided new, quantitative information about the system. Specifically the line connecting the transformation temperatures (line A, see Fig. 4) is ascribed to a kinetic barrier instead of a phase boundary. The same conclusion was previously argued in Refs. 20 and 24 concerning the transformation temperature. Here we observe that from room temperature measurements<sup>12,27</sup> phase V is known to be much denser than both phases III and II; in addition, structural and spectroscopic data for  $\text{CO}_2$ -V point to a lower entropy. These findings imply a positive slope of the expected  $T(P)$  phase boundary, as determined by the Clapeyron equation:  $dT/dP = \Delta V/\Delta S$ , where  $\Delta V$  and  $\Delta S$  are the volume and the entropy variation, respectively, between two coexisting phases at thermodynamic equilibrium. In contrast, line A shows a negative slope at least between 30 and 50 GPa. Moreover, the minimum exhibited by such a behavior around 50–55 GPa would indicate that the nonmolecular and molecular phases have the same specific volume, which is not the case; the volume difference between phase V and phase III (II) is equal to about 15% (8%–10%) at these pressures. The behavior of line A can be easily understood by regarding the III (II) to V transformation as a chemical reaction, which is reasonable due to the fact that the chemical bonds are completely reconstructed when  $\text{CO}_2$ -V is produced. Reactions may proceed when intermolecular distances reach a minimum; this condition can be achieved statically by increasing pressure or dynamically by increasing temperature. The negative slope of the line up to 50–55 GPa can thus be explained qualitatively. The amorphization of phase III occurring at higher pressures most probably tends to hinder the chemical reactivity due to a reduced molecular mobility, which is needed to allow reconstructed bonding, and a higher temperature is required to promote the reaction. The kinetic barrier character of line A, in turn, points to ascribing the entire underlined region of the phase diagram to the stability field of nonmolecular carbon dioxide instead of  $\text{CO}_2$ -III and/or  $\text{CO}_2$ -II. In other words, we suggest that the extended covalent solid recovered at room temperature, at least within the pressure range lying above 30 GPa, is more likely a stable than a metastable solid.

The line dividing phase III from phase II (line B in Fig. 4), was previously determined in the range between 14 and 30 GPa by externally heated DAC techniques,<sup>19</sup> and was linearly extrapolated to higher pressures. Like line A, it was suggested to be a kinetic barrier.<sup>19</sup> This implies that  $\text{CO}_2$ -III is a metastable phase in the conditions where it is observed; this agrees with the observation that only one  $P$ - $T$  path was found to achieve  $\text{CO}_2$ -III (i.e., it appears only via low temperature compression of phase I). The two kinetic barriers, line A and B, tend to converge with increasing pressure, intersecting around 43 GPa. This finding corresponds to the near simultaneity of the onset of phase II and V, which was observed specifically at 48–50 GPa. We point out that phase V can be formed from phases other than  $\text{CO}_2$ -II;  $\text{CO}_2$ -V can

be obtained directly from CO<sub>2</sub>-III when an abrupt increase of the laser heating power is employed.

The nonmolecular phase VI (Ref. 24) was not observed in our range of temperature and pressure. The frequency shifts of CO<sub>2</sub>-V (Fig. 5) are qualitatively in agreement with those reported by Iota *et al.*,<sup>20</sup> in the common pressure range. In addition we found them to be rather continuous; in contrast discontinuities in Raman frequencies together with an extra peak were observed and used to identify a new nonmolecular phase (CO<sub>2</sub>-VI) above 40 GPa in Ref. 24. We do not refute the existence of such a phase, since its kinetic barrier could simply be located at higher temperatures than those achieved in this work. Nonetheless, we point out that CO<sub>2</sub>-VI, which was suggested to be a precursor of the decomposition of carbon dioxide into molecular oxygen and carbon, was clearly evident only after having partially produced such decomposition. Additional work is needed to examine the effects of coexistence of the undecomposed material with the other species on the measured spectrum.

These results provide constraints on the *P-T* stability fields of solid phases of CO<sub>2</sub> in the region of the transformation to the nonmolecular phase (Fig. 6). The domains of phases I and IV are shown as in Ref. 19, while phase III appears to be metastable according to both experiment and theory. The domain of CO<sub>2</sub>-II is greatly reduced because of the lower phase boundary to CO<sub>2</sub>-V estimated on the basis of the following arguments. The entire region below the kinetic barrier to the nonmolecular solid lying above 30 GPa has to be assigned to the stable phase V, as observed above. As a consequence, the II-V phase boundary cannot intersect such a region. Furthermore, its slope has to be positive. Finally, at room temperature the low pressure limit of phase V

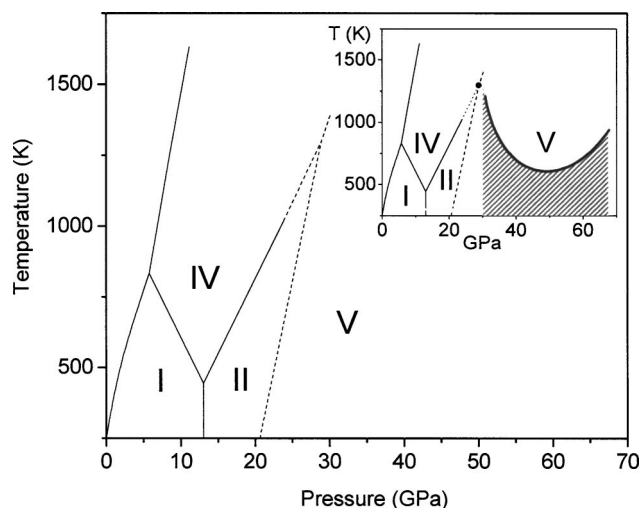


FIG. 6. Proposed stable phase diagram of carbon dioxide in the region of the transformation to nonmolecular CO<sub>2</sub>-V (see text). Inset: the domains of phases I and IV, delimited by continuous lines, are shown as in Ref. 19; the entire region (shaded area) below the kinetic barrier to the nonmolecular solid (thick continuous line, corresponding to the thick line reported in Fig. 4) has to be assigned to the stable phase V. By decompressing phase V, at room temperature, it starts to back-transform into CO<sub>2</sub>-I at 12 GPa, but it could also turn into a metastable state above this pressure, i.e., between 12 and 30 GPa (horizontal gray thick line). The dashed line represents the proposed phase boundary between CO<sub>2</sub>-II and CO<sub>2</sub>-V. A triple point between phases IV, II, and V is also expected (dot).

is about 12 GPa, where it starts to transform back into CO<sub>2</sub>-I, but it could also be metastable above this pressure, i.e., between 12 and 30 GPa; consequently we put the V to II phase transition, at room temperature, roughly in the middle of this pressure interval. A triple point between phases IV, II, and V is also expected. Additional work is needed to provide tighter bounds on the II-V phase boundary, but this is complicated by the strong kinetic barrier of the transitions. Theoretical calculations could help to overcome this difficulty.

We have demonstrated the capability of *in situ* Raman spectroscopy and laser heating technique in diamond anvil cells to quantitatively investigate the high *P-T* properties of carbon dioxide. Our study adds to the arsenal of new techniques for investigating molecular systems under extreme high *P-T* conditions. The study of such systems has important implications for understanding the interiors of planetary bodies of the outer Solar System.

## ACKNOWLEDGMENTS

This work was supported by DOE/BES, DOE/NNSA (CDAC), NSF, and the W. M. Keck Foundation. One of us (M.S.) acknowledges the European Union, supporting LENS under Contract No. RII3-CT-2003-506350. The authors are grateful to E. Gregoryanz and V. V. Struzhkin for their technical assistance in this study and their contribution to stimulating the scientific discussion.

- <sup>1</sup>K. Shimizu, K. Suhara, M. Ikumo, M. I. Eremets, and K. Amaya, *Nature* (London) **393**, 767 (1998).
- <sup>2</sup>K. Takemura, S. Minomura, O. Shimomura, and Y. Fujii, *Phys. Rev. Lett.* **45**, 1881 (1980).
- <sup>3</sup>M. I. Eremets, E. A. Gregoryanz, V. V. Struzhkin, H. K. Mao, R. J. Hemley, N. Mulders, and N. M. Zimmerman, *Phys. Rev. Lett.* **85**, 2797 (2000).
- <sup>4</sup>F. A. Gorelli, L. Ulivi, M. Santoro, and R. Bini, *Phys. Rev. Lett.* **83**, 4093 (1999).
- <sup>5</sup>M. Ceppatelli, M. Santoro, R. Bini, and V. Schettino, *J. Chem. Phys.* **113**, 5991 (2000).
- <sup>6</sup>M. Citroni, M. Ceppatelli, R. Bini, and V. Schettino, *Science* **295**, 2058 (2002).
- <sup>7</sup>L. Ciabini, M. Santoro, R. Bini, and V. Schettino, *J. Chem. Phys.* **116**, 2928 (2002); *Phys. Rev. Lett.* **88**, 085505 (2002).
- <sup>8</sup>T. J. Ahrens, in *Methods of Experimental Physics*, edited by C. G. Sammis and T. L. Henyey (Academic, Orlando, FL, 1987), Vol. 24, Part A, p. 185.
- <sup>9</sup>W. A. Bassett, *Rev. Sci. Instrum.* **72**, 1270 (2001).
- <sup>10</sup>G. Shen, M. L. Rivers, Y. Wang, and S. R. Sutton, *Rev. Sci. Instrum.* **72**, 1273 (2001).
- <sup>11</sup>B. Olinger, *J. Chem. Phys.* **77**, 6255 (1982).
- <sup>12</sup>C. S. Yoo, H. Cynn, F. Gygi, G. Galli, V. Iota, M. Nicol, S. Carlson, D. Hausermann, and C. Mailhot, *Phys. Rev. Lett.* **83**, 5527 (1999).
- <sup>13</sup>R. C. Hanson, *J. Phys. Chem.* **89**, 4499 (1985).
- <sup>14</sup>B. Kuchta and R. D. Eppers, *Phys. Rev. B* **38**, 6265 (1988); **47**, 14691 (1993).
- <sup>15</sup>K. Aoki, H. Yamawaki, and M. Sakashita, *Phys. Rev. B* **48**, 9231 (1993).
- <sup>16</sup>K. Aoki, H. Yamawaki, M. Sakashita, Y. Gotoh, and K. Takemura, *Science* **263**, 356 (1994).
- <sup>17</sup>R. Lu and A. M. Hofmeister, *Phys. Rev. B* **52**, 3985 (1995).
- <sup>18</sup>H. Olijnyk and A. P. Jephcoat, *Phys. Rev. B* **57**, 879 (1998).
- <sup>19</sup>V. Iota and C. S. Yoo, *Phys. Rev. Lett.* **86**, 5922 (2001).
- <sup>20</sup>V. Iota, C. S. Yoo, and H. Cynn, *Science* **283**, 1510 (1999).
- <sup>21</sup>S. Serra, C. Cavazzoni, G. L. Chiarotti, S. Scandolo, and E. Tosatti, *Science* **284**, 788 (1999).
- <sup>22</sup>J. Dong, J. K. Tomfohr, and O. F. Sankey, *Phys. Rev. B* **61**, 5967 (2000); *Science* **287**, 11a (2000); J. Dong, J. K. Tomfohr, K. Leinenweber, M. Somayazulu, and P. F. McMillan, *Phys. Rev. B* **62**, 14685 (2000).

- <sup>23</sup>B. Holm, R. Ahuja, A. Belonoshko, and B. Johansson, *Phys. Rev. Lett.* **85**, 1258 (2000).
- <sup>24</sup>O. Tschauer, H. K. Mao, and R. J. Hemley, *Phys. Rev. Lett.* **87**, 075701 (2001).
- <sup>25</sup>W. J. Nellis, A. C. Mitchell, F. H. Ree, M. Ross, N. C. Holmes, R. J. Trainor, and D. J. Erskine, *J. Chem. Phys.* **95**, 5268 (1991).
- <sup>26</sup>C. S. Yoo, V. Iota, and H. Cynn, *Phys. Rev. Lett.* **86**, 444 (2001).
- <sup>27</sup>C. S. Yoo, H. Kohlmann, H. Cynn, M. F. Nicol, V. Iota, and T. LeBihan, *Phys. Rev. B* **65**, 104103 (2002).
- <sup>28</sup>J.-H. Park, C. S. Yoo, V. Iota, H. Cynn, M. F. Nicol, and T. LeBihan, *Phys. Rev. B* **68**, 014107 (2003).
- <sup>29</sup>S. A. Bonev, F. Gygi, T. Ogitsu, and G. Galli, *Phys. Rev. Lett.* **91**, 065501 (2003).
- <sup>30</sup>H. K. Mao, P. M. Bell, J. W. Shaner, and D. J. Steinberg, *J. Appl. Phys.* **49**, 3276 (1978).